940 KSME International Journal, Vol. 13, No. 12, pp. 940~947, 1999

Fault Diagnosis of a Gearbox Using the Sliced Wigner Fourth Order Time Frequency Method Smoothed by a New Kernel Function

Sang-Kwon Lee*

(*Received July 8, 1999*)

The detection of impulsive signals embedded in the broadband noise is useful for the fault diagnosis of a gearbox. The sliced Wigner fourth-order time frequency method (SWFOTFM) has been used for the detection of impulsive signals embedded in the broadband noise. However, one disadvantage of SWFOTFM is that the non-oscillating cross-terms cannot be smoothed by conventional kernel functions. In this paper, a new kernel function is developed to reduce the non-oscillation cross-terms. The SWFOTFM using the new kernel function is successfully applied to the fault diagnosis of a gearbox.

Key Words : Gear, Fault, Wigner Higher-Order Distribution, Smoothing

1. Introduction

Recently, the bilinear class of time-frequency representations for impulsive signals has been applied successfully to the diagnosis of machinery (Lee and White, 1997a; Lee and White, 1998a). The bilinear class of time-frequency representations describes a signal's second order statistics as a function of time, and are suited for the analysis of non-stationary signals. Recently a good deal of research has been done on the analysis of non-stationary signals using higher-order spectra. Most of this research explores the linkage between HOS and time-frequency distributions. Gerr (Gerr, 1993) was the first to try to link higher-order statistical analysis with non-stationary analysis. He defined the 3rd order Wigner-Ville distribution for deterministic signals, which was later extended to an $n+1^{th}$ order moment-based Wigner-Ville distribution (Fonollosa and Nikias, 1993), referred to as WHOMS, that is based on the instantaneous $n+1^{th}$ order moment function.

The Wigner distribution has been used widely used because it has good time and frequency resolution properties (Cohen, 1995). However, the Wigner distribution for signals with multi-components has unwanted cross-terms, as does WHOMS for signals with multi-components. The number of cross-terms in WHOMS for signals with multi-components increases dramatically as the order increases (Lee and White, 1997b). In order to reduce the number of cross-terms, sliced WHOMS have been used. Sliced WHOMS has better detection performance of impulsive signals embedded in the broadband noise than the Wigner distribution. However, even sliced WHOMS cannot reduce the number of cross-terms for signals with multi-components at the same frequencies but different times, because there exist non-oscillating cross-terms which cannot be smoothed in the Wigner distribution by conventional kernel functions such as the exponential kernel function (Choi, 1989). In this paper, in order to smooth the non-oscillating cross-terms, SWHOMS weighted by a new kernel has been developed. The new kernel can smooth the non-oscillation cross-terms successfully. In general, impulsive signals occur but are embedded in the broadband noise when a gearbox has fatigue damage. Thus, the detection of impulsive signals is useful for the fault diagnosis of a gearbox. SWHOMS has been used for the detection of

* Department of Mechanical Engineering, Inha University

impulsive signals embedded in the broadband noise in a gearbox (Lee and White, 1997b). However, the non-oscillating cross-terms often hinder the detection of fault signals embedded in broadband. In this paper, SWHOMS using a new kernel function is applied to the early detection of gearbox damage.

2. Cross-Terms Analysis of WHOMS

The WHOMS of order n+1 is defined by Fonollosa (Fonollosa and Nikias, 1993) as

$$W(t, f_1, \cdots, f_n) = \int_{\tau_1} \cdots \int_{\tau_n} R^i_{n+1}(t, \tau_1, \cdots, \tau_n) \prod_{i=1}^{n} e^{-j2\pi f_i \tau_i} d\tau_i \quad (1)$$

where

$$R^i_{n+1}(t, \tau_1, \cdots, \tau_n) = s^*(t-\alpha) \prod_{i=1}^{n} s^{(*)^{i+1}}(t+\tau_i-\alpha) \quad (2)$$

The notation $(*)^i$ is introduced to denote alternating conjugations; for odd i, $(*)^i$ denotes conjugation, while for even i no conjugation occurs. while Equation (2) defines a set of possible distributions for different values of (, in order to extend most of the properties of the WVD, the lag centering condition has to be imposed, requiring that

$$\alpha = \frac{1}{n+1} \sum_{i=1}^{n} \tau_i \quad (3)$$

Thus, the WHOMS can be rewritten as

$$W(t, f_1, \cdots, f_n) = \int_{\tau_1} \cdots \int_{\tau_n} s^*\left(t - \frac{1}{n+1} \sum_{m=1}^{n} \tau_m\right) \cdot \prod_{i=1}^{n} s^{(*)^{i+1}}\left(t + \frac{n}{n+1}\tau_i - \frac{1}{n+1} \sum_{j=1, j\neq i}^{n} \tau_j\right) e^{-j2\pi f_i \tau_i} d\tau_i, \quad n = 1, 2, \cdots\cdots \quad (4)$$

By expressing $s(t)$ via an inverse Fourier Transform in Equation (4), an alternative definition for WHOMS is as follows:

$$W(t, f_1, \cdots, f_n) = \int_{\xi} S^*\left[\sum_{i=1}^{n} f_i + \frac{1}{n+1}\xi\right] \prod_{i=1}^{n} S^{(*)^{i+1}}\left[f_i - \frac{1}{n+1}\xi\right] e^{-j2\pi\xi t} d\xi \quad (5)$$

where n=1, n=2, and n=3 are the Wigner-Ville distribution (WVD), the Wigner third order-moment spectrum (WTOMS) and the Wigner fourth-order moment spectrum (WFOMS), respectively.

In the following, we present expressions for the cross-terms of the WVD, the WTOMS, and the WFOMS. Consider a signal $x(t)$ which consists of two components $s_a(t)$ and $s_b(t)$:

$$x(t) = s_a(t) + s_b(t) \quad (6)$$

Moreover, consider the following specific form of the two components :

$$s_a(t) = s(t-t_a) e^{j2\pi f_a t} \quad (7a)$$

$$s_b(t) = s(t-t_b) e^{j2\pi f_b t} \quad (7b)$$

where $s(t)$ is a prototype signal, t_a and t_b are time shifts, and f_a and f_b are frequency shifts. In general, the $n+1^{th}$ order Wigner distribution for two component signals is the sum of 2^{n+1} distributions, of which two are auto-terms and $2^{n+1}-2$ are cross-terms. A general expression for the cross-terms in the signal of the form (6) can be developed. These expressions are derived by simply substituting (6) and (7) into the definitions of the distributions, and performing simple but tedious manipulations (Lee, 1998b).

(i) The Wigner-Ville Distribution

$$W_2(t, f)_{p,q} = W_{ss}(t-t_m, f-f_m) e^{j2\pi(f_{d1}t + f\delta - f_m\delta)}, \quad p,q \in \{a, b\} \quad (8)$$

where $t_m = (t_p + t_q)/2$, $f_m = (f_p + f_q)/2$, $\delta = t_q - t_p$, $f_{d1} = f_q - f_p$, and $W_{ss}(t, f)$ is the WVD of $s(t)$. By way of an example of the above notation, $W_2(t, f)_{a,b}$ $(p=a, q=b)$ represents the cross-term between $s_a(t)$ and $s_b(t)$. The complete WVD of $x(t)$ is the sum of all components $W_2(t, f)_{p,q}$. From (8) it is clear that $W_2(t, f)_{a,b} = W_2(t, f)^*_{b,a}$, ensuring that the final distribution is real. Further, note that $W_2(t, f)_{a,a}$ and $W_2(t, f)_{b,b}$ are simply $W_{ss}(t, f)$ repositioned in the time-frequency plane.

It is also apparent that the cross-terms are oscillatory and that the rate of oscillation in the frequency direction (t=constant) is δ and the rate of oscillation in the time direction (f=constant) is f_{d1}. Thus, the cross-terms oscillate more rapidly the further apart the signal components are. Assuming smoothing is used to reduce the cross-terms, it is the rapid oscillations which are most easily attenuated, with the result that the

cross-terms between closely spaced components are more troublesome to attenuate than the cross-terms between distant components.

(ii) The Wigner third order moment spectrum

$$W_3(t, f_1, f_2)_{p,q,r} = W_{sss}(t-t_m, f_1+f_{d_2}/3-f_q, f_2 + f_{d_2}/3-f_r) \times e^{j2\pi(f_{d_2}t + f_1\delta_1 + f_2\delta_2 + f_d(\delta_m-\delta_1) + f_r(\delta_m-\delta_2) - f_p\delta_m)}, \quad p, q, \alpha \in \{a, b\} \tag{9}$$

where $t_m=(t_p+t_q+t_r)/3$, $f_{d_2}=(f_q+f_r-f_p)/3$, $\delta_1=t_p-t_r$, $\delta_m=(\delta_1+\delta_2)/3$, and $W_{sss}(t, f_1, f_2)$ is the WTOMS of $s(t)$. In this case the auto-terms ($p=q=r=a$ and $p=q=r=b$) are oscillatory due to the $e^{j2\pi f_{d_2}t}$ term, which is the only contributing exponential term. Further, the auto-terms are not located at the frequency points one might anticipate; for example, if we assume $p=q=r=a$, then $f_{d_2}=f_a/3$ and the auto-term is centered on the frequency pair ($f_1=2f_a/3$, $f_2=2f_b/3$).

(iii) The Wigner Fourth-Order Moment Spectrum

$$W_4(t, f_1, f_2, f_3)_{p,q,r,s} = W_{ssss}(t-t_m, f_1+f_{d_3}/4-f_q, f_2+f_{d_3}/4+f_r, f_3+f_{d_3}/4-f_s) \times e^{j2\pi(f_{d_3}t + f_1\delta_1 + f_2\delta_2 + f_3\delta_3 + f_d(\delta_m-\delta_1) - f_r(\delta_m-\delta_2) - f_s(\delta_m-\delta_3) - f_p\delta_m)}, \quad p, q, r, s\alpha \in \{a, b\} \tag{10}$$

where $f_{d_3}=(f_p+f_s-f_p-f_r)$, $\delta_3=t_p-t_s$, $\delta_m=(\delta_1+\delta_2+\delta_3)/4$, and $W_{ssss}(t, f_1, f_2, f_3)$ is the WFOMS of $s(t)$. In this case the auto-terms are non-oscillating and are located at the 'natural' position. To see this, take $p=q=r=s=a$, in which case $f_{d_3}=0$ and the auto-terms are centered on the frequency triplet ($f_1=f_a$, $f_2=f_a$, $f_3=f_a$).

The full WHOMS is a function of $n+1$ variables. This presents problems when attempting to display results, since the resulting plots exists in $n+2$ dimensional space. The computation of WHOMS also imposes a heavy computational burden as one is required to perform n dimensional FFTs for each time segment. For these reasons it is common to consider a subset of WHOMS called the principal slice (Lee and White, 1997b). The principal slice is defined as the only plane in which a single complex exponential appears as a Dirac delta. For the WTOMS this plane is defined by $f_1=f_2=f$ and $n=2$ in Equations (4) and (5). For WFOMS this plane is obtained by setting $f_1=-f_2=f_3=f$ and $n=3$. This slice generally includes both auto-terms and cross-terms and, as we show below, the number of cross-terms is significantly reduced.

In WTOMS, the only terms of (9) guaranteed to lie on the principal slice, *i. e.*, which satisfy the condition that the two frequency arguments are equal, are those such that $q=r$. This reduces the number of cross-terms from 6 to 2, and (9) becomes

$$W_3(t, f)_{p,q,r} = W_{sss}(t-t_m, f+f_{d_2}/3-f_q) e^{j2\pi(f_{d_2}+2f\delta-4/3f_m\delta)}, \quad p, q \in \{a, b\} \tag{11}$$

The remaining two cross-terms $W_3(t, f)_{a,b,b}$ and $W_3(t, f)_{b,a,a}$ are centered on $((2t_a+t_b)/3, (f_a+f_b)/3)$ and $((t_a+2t_b)/3, (f_a+f_b)/3)$, respectively.

By taking the principal slice of WFOMS, the only terms in (10) which are guaranteed to remain are those for which $r=p$ and $s=q$, so the original 14 cross-terms in WFOMS reduce to only two in its principal slice. The principal slice version of (10) is

$$W_4(t, f)_{p,q} = W_{sss}(t-t_m, f-(f_p+f_q)/2) e^{j2\pi(2f_{d_3}t+2f\delta-2f_m\delta)}, \quad p, q \in \{a, b\} \tag{12}$$

This should be compared with the corresponding expression for the standard Wigner distribution (8). In both cases the cross-terms are located mid-way between the auto-terms and oscillate at rates proportional to the separation of signal components.

While (12) describes all the terms which necessarily lie on the principal slice, if the two frequency shifts are equal, *i. e.*, $f_a=f_b$, then $f_{d_3}=0$, in which all the elements of (12) lie on the principal slice, and we can write

$$W_4(t, f)_{p,q,r,s} = W_{ssss}(t-t_m, f-f_p) e^{j2\pi(t_p-t_q+t_r-t_s)(f-f_p)} \tag{13}$$

These components are located in time at quarter intervals between t_a and t_b. None of the terms in (13) oscillates as a function of time; further, for terms satisfying $t_p-t_q+t_r-t_s=0$, (13) is completely non-oscillatory. These non-oscillatory terms are difficult to distinguish from the auto-terms; for example, conventional smoothing will fail to attenuate them (Lee and White, 1997b).

3. Smoothing of Non-Oscillating Cross-Terms in the Sliced WHOMS

In order to smooth effectively the non-oscillating cross-terms in the sliced WHOMS, consider the frequency version of the WVD :

$$W(t, f)=\int_{\xi} S^*\left[f+\frac{1}{2}\xi\right]S\left[f-\frac{1}{2}\xi\right] e^{-j2\pi\xi t}d\xi \tag{14}$$

The pseudo-Wigner distribution (PWD) (Classen, et al., 1980), can be written using the frequency domain windowing function $H(\xi/2)$ as follows:

$$W_{pw}(t, f)=\int_{\xi} H(-\frac{\xi}{2})H^*\left(\frac{\xi}{2}\right)S^*\left[f+\frac{1}{2}\xi\right]S\left[f-\frac{1}{2}\xi\right] e^{-j2\pi\xi t}d\xi=\frac{1}{2}\int_{\xi'} H(-\xi')H^*(\xi')S^* (f+\xi')S(f-\xi')e^{-j2\pi\xi'(2t)}d\xi' \tag{15}$$

where $\xi'=\xi/2$. Using convolution, Eq. (15) may be written as follows:

$$W_{pw}(t, f)=s_h^*(f, 2t)\underset{t}{*}s_h(f, 2t) \tag{16}$$

where $s_h(f, t)$ is the short time Fourier transform (STFT) (Cohen, 1995), Therefore, the PWD can be written as

$$\begin{aligned} W_{pw}(t, f)&=s_h^*(f, 2t)\underset{t}{*}s_h(f, 2t)\\ &=\int_{-\infty}^{\infty} s_h^*(f, 2t-\tau)\,d\tau\\ &=\int_{-\infty}^{\infty} s_h^*(f, t+\tau)s_h(f, t-\tau)\,d\tau \end{aligned} \tag{17}$$

In order to emphasige the auto-terms of the PWD for a multi-component signal, a window function $\gamma(\tau)$ can be incorporated into Eq. (17), and the smoothed pseudo Wigner distribution (SPWD) can be developed as follows:

$$W_{2,spw}(t, f)=\int_{-\infty}^{\infty}\gamma(\tau)s_h^*(f, t+\tau)s(f, t-\tau)\,d\tau \tag{18}$$

Therefore, using the ambiguity plane (ξ, τ) (Claasen, 1980), the kernel function for this window function $\gamma(\tau)$ can be developed as follows:

$$\Phi(\tau, \xi)=\gamma(\tau)\underset{\tau}{*}A_{g,sp}(\xi, \tau) \tag{19}$$

where $A_{g,sp}(\xi, \tau)$ is the general ambiguity function associated with the spectrogram of signal $s(t)$. We refer to this kernel function as the γ method. In Eq. (18), when $\gamma(\tau)=1$, the SPWD becomes the WVD, and when $\gamma(\tau)=\delta(\tau)$, the SPWD becomes the spectrogram. Therefore, in order to smooth the cross-terms of the WVD for the signal of the form of Eq. (6), the duration T_γ for $\gamma(\tau)$ needs to be selected in accordance with

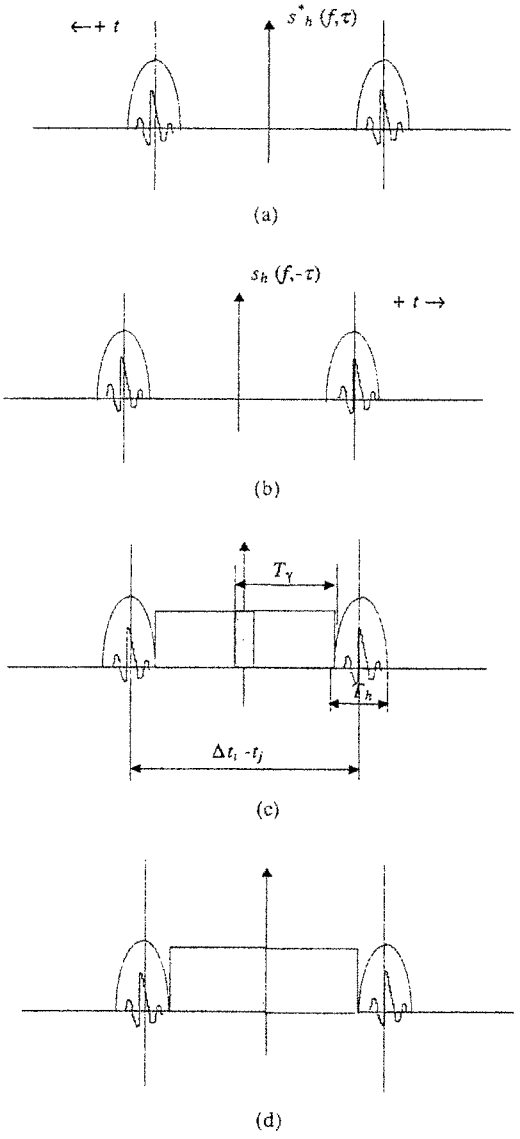

Fig. 1 Illustrate the proper width of the $\gamma(\tau)$ window function (a) convolving signal $s_h^*(t)$ (b) convolving of signal $s_h(t)$ (c) $T_\gamma > t_i - t_j/2 - T_h$ (d) $T_\gamma < t_i - t_j/2 - T_h$

$$T_h < T < \min_{i,j} \frac{\Delta t_{ij} - t_j}{2} - T_h \qquad (20)$$

where t_i and t_j are the temporal positions of the signal components, and T_h is the duration of $h(t)$.

An intuitive justification for Eq. (20) can be seen with reference to Fig. 1. Consider the convolution of $s_h(f, 2t)$ and $s_h^*(f, 2t)$ using a rectangular window $\gamma(t)$. In order that only the auto-terms are convolved, Eq. (20) should be satisfied as shown in Fig. 1(c). Otherwise, the cross-terms will also be included in the convolution, as shown in Fig. 1(d).

The SPWD is obtained by convolving two signals $s_h(f, 2t)$ and $s_h^*(f, 2t)$ with respect to time and using the γ-method to smooth the cross-terms in Equation (18). Similarly, a smoothed version of SWFOMS also can be obtained by the convolution of two SPWD $W_{2,spw}(f, 2t)$ and $W_{2^*,spw}(f, 2t)$ with respect to time as follows:

$$W_{4,spw}(t, f) = \frac{1}{2}\int_{\tau} \gamma(\tau) \cdot W_{2,spw}(f, t+\tau) \cdot W_{2,spw}^*(f, t-\tau)\, d\tau \qquad (21)$$

Therefore, a general form of the smoothed version of sliced WHOMS can be obtained as follows:

$$W_{n+3,spw}(t, f) = \frac{1}{2}\int_{\tau} \gamma(\tau) \cdot W_{n+,spw}(f, t+\tau) \cdot W_{n+1,spw}^*(f, t-\tau)\, d\tau,\ n=1, 3, 5, \cdots \qquad (22)$$

where $W_{n+1,spw}(t, f)$ is the smoothed pseudo-Wigner distribution ($n=1$), or the smoothed version of the sliced WHOMS ($n=3, 5, \cdots$).

4. Numerical Example

The previons theoretical observations are verified via a simulation, the results of which are shown in Fig. 2. In Fig. 2 (a), The SWFOMS is computed for a 128 point time series at an assumed sampling rate of 100 Hz. The signal contains two components occurring at different times, 0.2s and 1.08 s, but at the same frequency, 12.5 Hz. In this case there are three sets of cross-terms, in contrast to the WVD which would only generate a single set of cross-terms as shown in

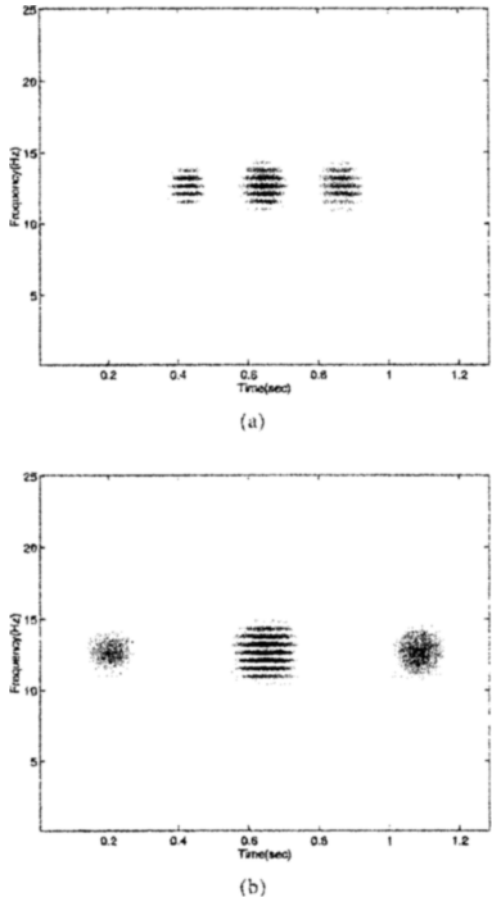

Fig. 2 Comparison between the WVD and SWFOMS for the two components signal centred at 0.2s and 1.08 s with 12.5Hz (a) SWFOMS (b) WVD

Fig. 2(b). The SWFOMS cross-terms appear at quarter intervals between the two components. The off-center cross-terms at 1/4 and 3/4 of the interval are oscillatory albeit only in the frequency direction. However, the cross-terms appearing at mid-point contains both an oscillatory element and a non-oscillating element. Figure 3 shows the results of applying the exponential kernel to the data depicted in Fig. 2 (a). The results of this simulation are less satisfying since the exponential kernel is poorly suited to removing cross-terms between vertically and horizontally displaced components (since it is impossible to smooth non-oscillating cross-terms by the exponential kernel function). The effectiveness of smoothing the SWFOMS using the

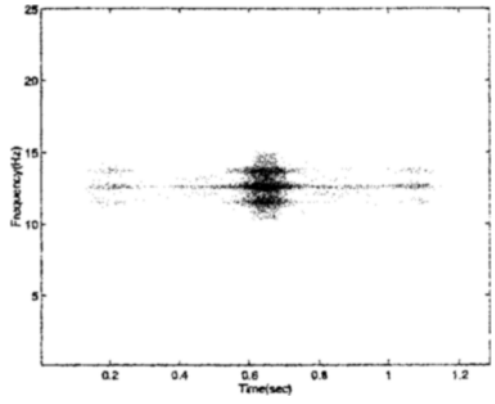

Fig. 3 The SWFOMS using an exponential kernel for the two components signal centred at 0.2s and 1.08 s with 12.5Hz

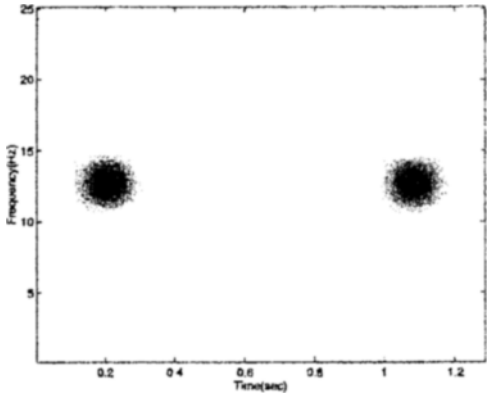

Fig. 4 The SWFOMS using the γ-method for the two components signal centred at 0.2s and 1.08 s with 12.5Hz

γ-method is again demonstrated via a simple simulation. Figure 4 depicts the SWFOMS calculated for the same data set as used to compute Fig. 2 using the γ-method. In this case the sampling frequency is 100Hz, the number of samples is 512 for fs, and $t_i - t_j = 0.88$ s. 0.12 s is used as the width of the window for $\gamma(\tau)$, and 0.64 s is the duration of the sliding window $h(\tau)$ with a bandwidth of 50Hz. According to these results, the non-oscillating cross-terms can be eliminated as shown in Fig. 4.

5. Application

In general, vibration signals from a gearbox under normal conditions consist of tonal components related to the rotation speed and broadband noise, while under faulty condition, impulsive signals are added to them (Stewart, 1977 and Randall 1982). These impulsive signals may be due to a change of stiffness or mass in the system or due to impact. Therefore, if we detect impulsive signals exactly, we can diagnose the faults and characterise the change in dynamic characteristics of the system. When the damage is fully developed, the impulsive signal is visible in the time domain (Lee, 1999). However, at early stages of damage, it is often difficult to detect these impulsive signals because they are embedded in the normal vibration signal. Thus, normal vibration signal becomes background noise. The human ear can sometimes detect these impulsive signals, and a skilled engineer can both detect and characterise the fault. Therefore, to aid fault detection in gearbox, it is valuable to enhance impulsive signals by removing or reducing the background noise prior to further processing. This pre-processed signal can proceed based on several signal-processing techniques. As one pre-processing method, time domain averaging (Stewart, 1977) has been used, but it requires the reference signal to be synchronised to the rotating speed. However, when a reference signal is unavailable, the two-stage Adaptive Line Enhancer (ALE) achieves this aim (Lee and White, 1998a).

Figure 5(a) shows the vibration signal measured on the tooth of a faulty gear of the pinion. This data is the same as that used by Dalpiaz (Dalpiaz, et al., 1996), and was supplied by one of the authors. The speed of the wheel is 1500 rpm, while the number of samples per rotation is 1024 (We note that This is not time-averaged data). From Fig. 5(a) it is difficult to see the impulsive signal due to the fault because of the large amplitude tonal signals, which constitute the gear meshing frequency and its harmonic frequencies. In this gear the pinion has 28 teeth and the wheel has 55. Thus the 55^{th} order represents the fundamental meshing frequency. In order to remove the fundamental and harmonics of the tooth meshing frequency, the two-stage ALE is employed. The enhanced impulsive signal

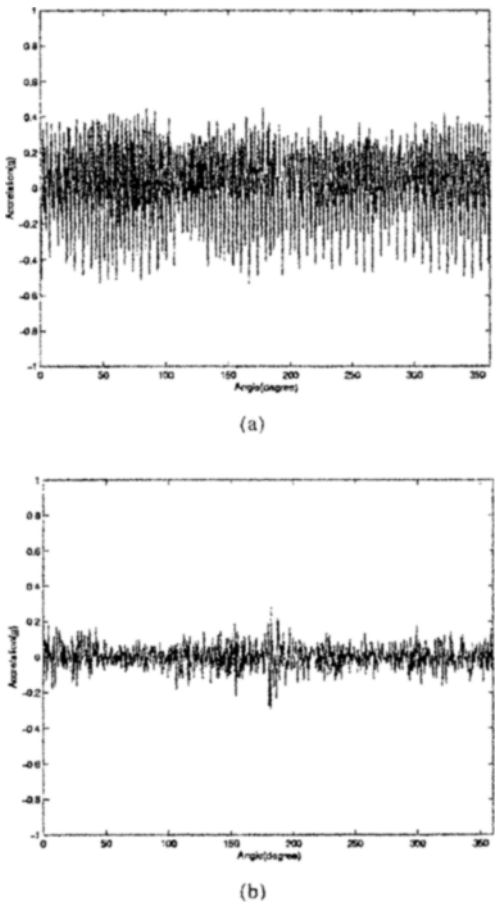

Fig. 5 Using Two-Stage ALE (Adaptive Line Enhancer) the detection of impulsive signals due to a faulty gear (a) Raw signal: vibrational signal measured on a gear (b) Enhanced impulsive signal by using Two-Stage ALE.

generated by faults is shown in Fig. 5(b). In order to see both the time and frequency information simultaneously, the Wigner-Ville Distribution using an exponential kernel is applied to the raw signal as shown in Fig. 6(a). The mashing frequency (the 55 order) and its harmonics are dominant because the impulsive signal is hidden. After pre-processing the signal using the two-stage ALE and then applying the Wigner-Ville-Distribution with an exponential kernel, Fig. 6 (b) is obtained, in which the effect of the impulsive signal is visible. However, the frequency components are still interfered by the residue of the cross-terms. The SWFOMS using a γ-method

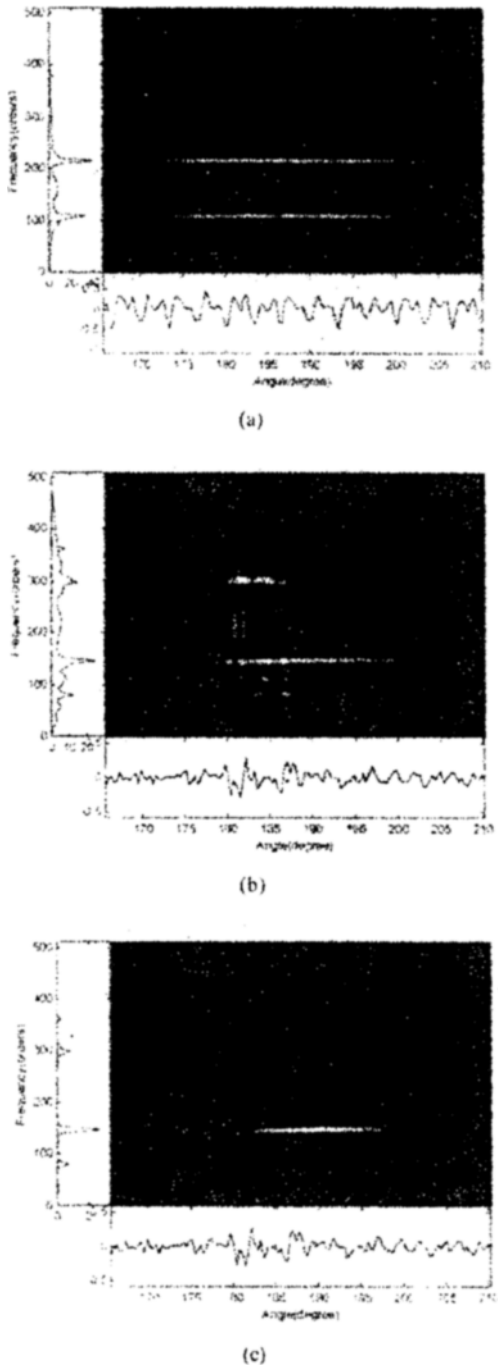

Fig. 6 Time-frequency analysis of vibrational data measured on the gearbox (a) the WVD using an exponential kernel for raw vibrational data measured on a gear (b) the WVD using an exponential kernel for enhanced signal (c) the SWFOMS using the γ-method for enhanced signal

for this enhanced signal creates a clearer representation of this fault signal as shown in Fig. 6(c). From this result, one can conclude that the gear fault occurs at shaft angles of 180° and at 110±28 orders of shaft rotating speed. This appears to result from an increase in the sidebands of the 2nd meshing frequency of the wheel gear. This fault at shaft angle 180° also includes the ghost[12] component at order 300.

6. Conclusion

In this paper, time-frequency methods using higher-order statistics are discussed. The WHOMS is a general expansion of the conventional Wigner-Ville Distribution and preserves its properties. In both higher-order time frequency analyses, as the order increases, the number of cross-terms also increases. This problem can be reduced using the principal sliced WHOMS. However, for horizontally or vertically displaced components, the sliced WHOMS suffers from non-oscillating cross-terms, which lead to failure of the smoothing method for the reduction of cross-terms. In order to smooth non-oscillating cross-terms, the γ-method for sliced WHOMS can be used. The SWFOMS using the γ-method is a more useful tool for the detection of impulsive signals embedded in broadband noise, and can be applied to the effective analysis of faults in a gearbox.

References

Choi, H. I. and Williams, W., 1989, "Improved Time-Frequency Representation of Multiple Component Signal Using Exponential Kernel," *IEEE Transaction on ASSP*, Vol. 37, pp. 862 ~871.

Claasen, A. C. M. and Mecklenbrauker, W. F. G., 1980, "The Wigner Distribution-A Tool for Time-Frequency Signal Analysis : part Ⅰ, Ⅱ, Ⅲ," *Phil. J. Res.*, Vol. 35, pp. 217~389.

Cohen, L., 1995, *Time-Frequency Analysis*. Prentice Hall.

Dalpiaz, G., Dalpiaz, A. and Rubini, R., 1996, "Dynamic Modelling of Gear System for Condition Monitoring and Diagnostics," *Proceedings of the Congress of Technical Diagnostics-KDT Gdansk*, Poland, September, pp. 185~192.

Fonollosa, J. R. and Nikias, C. L., 1993, "Wigner-Higher-Order Moment Spectra Definition, Properties, Computation and Application to Transient Signal Analysis," *IEEE Transaction on Signal Processing*, Vol. 41, pp. 245~266.

Gerr, N. L., 1998, "Introducing the Third-Order Wigner Distribution," *Proceeding of IEEE*, Vol. 13, pp. 290~292.

Lee, S. K. and White, P. R., 1997a, "Fault identification for rotating machinery using adaptive signal processing and time-frequency analysis" *The ASME Design Engineering Technical Conferences*, DETC97/VIB-4236, the 16th Biennial Conference on Mechanical Vibration and Noise, Symposium on Time-Frequency and Wavelet Analysis, Sacramento, California, USA, September.

Lee, S. K. and White, P. R., 1997b, "Fault diagnosis of rotating machinery using Wigner Higher Order Moment Spectra," *Mechanical Systems and Signal Processing*, Vol. 11, pp. 637 ~650.

Lee, S. K. and White, P. R., 1998a, "The Enhancement of Impulsive Noise and Vibration Signals for Fault Detection in Rotating and Reciprocating Machinery," *Journal of Sound and Vibration*, Vol. 217, No. 3, pp. 484~505.

Lee, S. K., 1998b "Adaptive Signal Processing and Higher Order Time Frequency Analysis and Their Application to Condition Monitoring," Ph. D. thesis, ISVR, The University of Southampton, U. K.

Lee, S. K., 1999, "Application of the L-Wigner Distribution to the Diagnosis of Local Defects of Gear tooth," *KSME International Journal*, Vol. 13, No. 2, pp. 144~157.

Randall, B., "A New Method of Modeling Gear Faults," 1982, *ASME Trans. Journal of Mechanical Design*, Vol. 1, pp. 259~267.

STEWART, M., 1977, "Some Useful Data Analysis Techniques for Gearbox Diagnostics," *ISVR University of Southampton Report*, MHM/R/10/77.